# Supplementary Materials

# Plasma N-glycome shows continuous deterioration as the diagnosis of insulin resistance approaches

Ana Cvetko[1]*, Massimo Mangino[2,3]*, Marko Tijardović[1], Domagoj Kifer[1], Mario Falchi[2], Toma Keser[1], Markus Perola[4], Tim D Spector[2], Gordan Lauc[1,5], Cristina Menni[2]*, Olga Gornik[1]*

[1]Faculty of Pharmacy and Biochemistry, University of Zagreb, Zagreb 10000, Croatia

[2]Department of Twin Research and Genetic Epidemiology, King's College London, Westminster Bridge Road, SE17EH London, UK

[3]NIHR Biomedical Research Centre at Guy's and St Thomas' Foundation Trust, London SE1 9RT, UK

[4]National Institute for Health and Welfare, Helsinki, Finland

[5]Genos Glycoscience Research Laboratory, Zagreb 10000, Croatia

*These authors contributed equally

Corresponding author:

Olga Gornik

ogornik@pharma.unizg.hr

Faculty of Pharmacy and Biochemistry, University of Zagreb

A. Kovačića 1, 10 000 Zagreb, Croatia

**Supplementary Table 1** Abbreviation and description of all glycan structures complementary to every plasma glycan peak.*

| ***Sample*** | ***Glycan peak*** | ***Glycan structure abbreviation*** | ***Glycan structure description*** | ***Glycan peak abundance formula*** |
|---|---|---|---|---|
| plasma | GP1 | FA2 | core fucosylated, biantennary | GP1 / GP * 100 |
| plasma | GP2 | FA2B; M5 | core fucosylated, biantennary with bisecting GlcNAc;<br>oligomannose | GP2 / GP * 100 |
| plasma | GP3 | A2BG1 | monogalactosylated, biantennary with bisecting GlcNAc | GP3 / GP * 100 |
| plasma | GP4 | FA2[6]G1 | core fucosylated and monogalactosylated, biantennary | GP4 / GP * 100 |
| plasma | GP5 | FA2[3]G1 | core fucosylated and monogalactosylated, biantennary | GP5 / GP * 100 |
| plasma | GP6 | FA2[6]BG1 | core fucosylated and monogalactosylated, biantennary with bisecting GlcNAc | GP6 / GP * 100 |
| plasma | GP7 | M6;<br>FA2[3]BG1 | oligomannose;<br>core fucosylated and monogalactosylated, biantennary with bisecting GlcNAc | GP7 / GP * 100 |
| plasma | GP8 | A2G2 | digalactosylated, biantennary | GP8 / GP * 100 |
| plasma | GP9 | A2BG2 | digalactosylated, biantennary with bisecting GlcNAc | GP9 / GP * 100 |
| plasma | GP10 | FA2G2 | core fucosylated, digalactosylated, biantennary | GP10 / GP * 100 |
| plasma | GP11 | FA2BG2 | core fucosylated, digalactosylated, biantennary with bisecting GlcNAc | GP11 / GP * 100 |
| plasma | GP12 | M7;<br>A2G2S1;<br>A1M4G1S1;<br>A2BG1S1 | oligomannose;<br>digalactosylated, monosialylated, biantennary;<br>tetramannosylated, monogalactosylated, monosialylated, monoantennary;<br>monogalactosylated, monosialylated, biantennary with bisecting GlcNAc | GP12 / GP * 100 |
| plasma | GP13 | FA2G1S1;<br>FA2BG1S1 | core fucosylated, monogalactosylated and monosialylated biantennary;<br>core fucosylated, monogalactosylated and monosialylated biantennary with bisecting GlcNAc | GP13 / GP * 100 |
| plasma | GP14 | A2G2S1 | digalactosylated and monosialylated biantennary | GP14 / GP * 100 |
| plasma | GP15 | A2BG2S1 | digalactosylated and monosialylated biantennary with bisecting GlcNAc | GP15 / GP * 100 |
| plasma | GP16 | FA2G2S1 | core fucosylated, digalactosylated and monosialylated biantennary | GP16 / GP * 100 |
| plasma | GP17 | FA2BG2S1 | core fucosylated, digalactosylated and monosialylated biantennary with bisecting GlcNAc | GP17/ GP * 100 |
| plasma | GP18 | A2G2S2;<br>FA2G2S2 | digalactosylated and disialylated biantennary;<br>core fucosylated, digalactosylated and disialylated biantennary | GP18 / GP * 100 |

| | | | | |
|---|---|---|---|---|
| plasma | GP19 | M9 | oligomannose | GP19 / GP * 100 |
| plasma | GP20 | A2G2S2 | digalactosylated and disialylated biantennary | GP20 / GP * 100 |
| plasma | GP21 | A2G2S2;<br>A3G3S1;<br>FA2G2S2;<br>A2BG2S2;<br>A3F1G3S1 | digalactosylated and disialylated biantennary;<br>trigalactosylated and monosialylated triantennary;<br>core fucosylated, digalactosylated and disialylated biantennary;<br>digalactosylated and disialylated biantennary with bisecting GlcNAc;<br>antennary fucosylated, trigalactosylated and monosialylated triantennary | GP21 / GP * 100 |
| plasma | GP22 | FA2G2S2 | core fucosylated, digalactosylated and disialylated biantennary | GP22 / GP * 100 |
| plasma | GP23 | FA2BG2S2 | core fucosylated, digalactosylated and disialylated biantennary with bisecting GlcNAc | GP23 / GP * 100 |
| plasma | GP24 | A3G3S2;<br>A3F1G3S1 | trigalactosylated and disialylated triantennary;<br>antennary fucosylated, trigalactosylated and monosialylated triantennary | GP24 / GP * 100 |
| plasma | GP25 | A3G3S2;<br>FA2F1G2S2;<br>A3F1G3S2 | trigalactosylated and disialylated triantennary;<br>core fucosylated, antennary fucosylated, digalactosylated and disialylated biantennary;<br>antennary fucosylated, trigalactosylated and disialylated triantennary | GP25 / GP * 100 |
| plasma | GP26 | A3G3S2;<br>FA3G3S2 | trigalactosylated and disialylated triantennary;<br>core fucosylated, trigalactosylated and disialylated triantennary | GP26 / GP * 100 |
| plasma | GP27 | A3F1G3S2;<br>A3G3S3 | antennary fucosylated, trigalactosylated and disialylated triantennary;<br>trigalactosylated and trisialylated triantennary | GP27 / GP * 100 |
| plasma | GP28 | A3G3S3;<br>A3F1G3S2 | trigalactosylated and trisialylated triantennary;<br>antennary fucosylated, trigalactosylated and disialylated triantennary | GP28 / GP * 100 |
| plasma | GP29 | A3G3S3;<br>A3F1G3S2 | trigalactosylated and trisialylated triantennary;<br>antennary fucosylated, trigalactosylated and disialylated triantennary | GP29 / GP * 100 |
| plasma | GP30 | A3G3S3;<br>A3F1G3S3 | trigalactosylated and trisialylated triantennary;<br>antennary fucosylated, trigalactosylated and trisialylated triantennary | GP30 / GP * 100 |
| plasma | GP31 | FA3G3S3;<br>A3G3S3 | core fucosylated, trigalactosylated and trisialylated triantennary;<br>trigalactosylated and trisialylated triantennary | GP31 / GP * 100 |
| plasma | GP32 | A3G3S3 | trigalactosylated and trisialylated triantennary | GP32 / GP * 100 |
| plasma | GP33 | A3F1G3S3 | antennary fucosylated, trigalactosylated and trisialylated triantennary | GP33 / GP * 100 |
| plasma | GP34 | FA3G3S3;<br>A4G4S3 | core fucosylated, trigalactosylated and trisialylated triantennary;<br>tetragalactosylated and trisialylated tetraantennary | GP34 / GP * 100 |
| plasma | GP35 | FA3F1G3S3;<br>A4F1G4S3 | core fucosylated, antennary fucosylated, trigalactosylated and trisialylated triantennary;<br>antennary fucosylated, tetragalactosylated and trisialylated tetraantennary | GP35 / GP * 100 |

| | | | | |
|---|---|---|---|---|
| plasma | GP36 | A4G4S3;<br>A4F1G4S3 | tetragalactosylated and trisialylated tetraantennary;<br>antennary fucosylated, tetragalactosylated and trisialylated tetraantennary | GP36 / GP * 100 |
| plasma | GP37 | A4G4S4;<br>A4F1G4S3 | tetragalactosylated and tetrasialylated tetraantennary;<br>antennary fucosylated, tetragalactosylated and trisialylated tetraantennary | GP37 / GP * 100 |
| plasma | GP38 | A4G4S4;<br>A4F1G4S4;<br>A4F1G4S3 | tetragalactosylated and tetrasialylated tetraantennary;<br>antennary fucosylated, tetragalactosylated and tetrasialylated tetraantennary;<br>antennary fucosylated, tetragalactosylated and trisialylated tetraantennary | GP38 / GP * 100 |
| plasma | GP39 | A4F1G4S4;<br>A4F2G4S4 | antennary fucosylated, tetragalactosylated and tetrasialylated tetraantennary;<br>antennary difucosylated, tetragalactosylated and tetrasialylated tetraantennary; | GP39 / GP * 100 |

*structure abbreviations – all N-glycans have two core *N*-acetylglucosamines (GlcNAcs); F at the start of the abbreviation indicates a core-fucose α1,6-linked to the inner GlcNAc; Mx, number (x) of mannose on core GlcNAcs; Ax, number of antenna (GlcNAc) on trimannosyl core; A2, biantennary with both GlcNAcs as β1,2-linked; A3, triantennary with a GlcNAc linked β1,2 to both mannose and the third GlcNAc linked β1,4 to the α1,3 linked mannose; A4, GlcNAcs linked as A3 with additional GlcNAc β1,6 linked to α1,6 mannose; B, bisecting GlcNAc linked β1,4 to β1,3 mannose; G(x), number (x) of β1,4 linked galactose on antenna; F(x), number (x) of fucose linked α1,3 to antenna GlcNAc; S(x), number (x) of sialic acids linked to galactose

**Supplementary Table 2** Formulas for plasma N-glycome derived glycan traits calculation. 16 derived traits are calculated out of 39 directly measured initial plasma glycan traits.

| ***Plasma N-glycome derived trait*** | ***Formula*** |
|---|---|
| Low branching (mono- and biantennary glycans) (LB) | GP1+GP2+GP3+GP4+GP5+GP6+GP8+GP9+GP10+GP11+0.5xGP12+GP13+GP14+ GP15+GP16+GP17+GP18+GP20+GP21+GP22+GP23 |
| High branching (tri- and tetraantennary glycans) (HB) | GP24+GP25+GP26+GP27+GP28+GP29+GP30+GP31+GP32+GP33+GP34+ GP35+GP36+GP37+GP38+GP39 |
| Agalactosylation (G0) | GP1+GP2 |
| Monogalactosylation (G1) | GP3+GP4+GP5+GP6+GP13 |
| Digalactosylation (G2) | GP8+GP9+GP10+GP11+0.5xGP12+GP14+GP15+GP16+GP17+GP18+GP20+GP21+GP22+GP23 |
| Trigalactosylation (G3) | GP24+GP25+GP26+GP27+GP28+GP29+GP30+GP31+GP32+GP33+GP34+ GP35 |
| Tetragalactosylation (G4) | GP36+GP37+GP38+GP39 |
| Neutral glycans (S0) | GP1+GP2+GP3+GP4+GP5+GP6+GP8+GP9+GP10+GP11 |
| Monosialylation (S1) | 0.5xGP12+GP13+GP14+GP15+GP16+GP17 |
| Disialylation (S2) | GP18+GP20+GP21+GP22+GP23+GP24+GP25+GP26+GP27 |
| Trisialylation (S3) | GP28+GP29+GP30+GP31+GP32+GP33+GP34+GP35+GP36 |
| Tetrasialylation (S4) | GP37+GP38+GP39 |
| Incidence of bisecting GlcNAc (B) | GP2+GP3+GP6+GP9+GP11+GP15+GP17+GP23 |
| Antennary fucosylation (AF) | GP27+GP33+GP35+GP39 |
| Core fucosylation (CF) | GP1+GP2+GP4+GP5+GP6+GP10+GP11+GP13+GP16+GP17+GP22+GP23+GP31+GP34+GP35 |
| Oligomannose glycans (M) | GP7+0.5xGP12+GP19 |

**Supplementary Table 3** The development of IR/T2DM induces significant changes in directly measured plasma N-glycans and plasma N-glycome derived traits in the TwinsUK cohort. Calculated effect size (natural logarithm of difference in relative area) for each of statistically significant derived trait is listed along with corresponding adjusted p-values.

| ***Plasma N-glycome peak*** | ***Effect size*** | ***95% Confidence interval*** | ***Adjusted p value*** |
|---|---|---|---|
| **GP10** | -0.14 | (-0.2134, -0.3488) | $3.99 \times 10^{-03}$ |
| **GP16** | -0.08 | (-0.126, -0.2096) | $9.38 \times 10^{-04}$ |
| **GP18** | -0.08 | (-0.1154, -0.1922) | $9.38 \times 10^{-04}$ |
| **GP19** | 0.07 | (0.0366, 0.1086) | $9.38 \times 10^{-04}$ |
| **GP20** | 0.04 | (0.0089, 0.0443) | $4.48 \times 10^{-02}$ |
| **GP26** | 0.09 | (0.0446, 0.1367) | $1.05 \times 10^{-03}$ |
| **GP32** | 0.15 | (0.0957, 0.2487) | $9.52 \times 10^{-06}$ |
| **GP34** | 0.12 | (0.0636, 0.1859) | $9.38 \times 10^{-04}$ |
| ***Plasma N-glycome derived trait*** | ***Effect size*** | ***95% Confidence interval*** | ***Adjusted p value*** |
| **LB** | -0.01 | (-0.0169, -0.0266) | $2.84 \times 10^{-02}$ |
| **HB** | 0.04 | (0.0113, 0.0541) | $2.84 \times 10^{-02}$ |
| **G3** | 0.04 | (0.0111, 0.0549) | $2.84 \times 10^{-02}$ |
| **S1** | -0.04 | (-0.0537, -0.0899) | $1.07 \times 10^{-03}$ |
| **S3** | 0.05 | (0.0136, 0.0614) | $2.84 \times 10^{-02}$ |

**Supplementary Table 4** Average age of both cases and controls for each temporal group created around the diagnosis.

| ***Temporal group according to disease diagnosis*** | ***cases*** *age (mean ± SD), years* | ***controls*** *age (mean ± SD), years* | ***case*** *samples, N* | ***control*** *samples, N* |
|---|---|---|---|---|
| pre 8-10 years | 53.35 ± 8.91 | 53.36 ± 8.97 | 23 | 115 |
| pre 5-7 years | 54.78 ± 8.40 | 54.77 ± 8.40 | 37 | 185 |
| pre 2-4 years | 53.98 ± 8.36 | 53.72 ± 8.05 | 40 | 198 |
| post 0-2 years | 59.69 ± 8.35 | 59.02 ± 7.60 | 49 | 237 |

**Supplementary Table 5** ROC curve point data showing specificity, sensitivity, Youden's index, true neutrals (tn), true positives (tp), false negatives (n) and false positives (fp) for each cut-off threshold of the three tested models. Data for each model is listed on a separate document sheet. Available as a separate file.

**Supplementary Table 6** The development of T2DM induces significant changes in directly measured plasma N-glycans in the FINRISK cohort. Calculated effect size (natural logarithm of difference in relative area) for each of statistically significant derived trait is listed along with corresponding adjusted p-values.

| *Plasma N-glycome peak* | *Effect size* | *95% Confidence interval* | *Adjusted p value* |
|---|---|---|---|
| **GP10** | -0.33 | (-0.8355, 0.1159) | $5.92 \times 10^{-01}$ |
| **GP16** | 0.06 | (-0.3139, 0.4017) | $7.68 \times 10^{-01}$ |
| **GP18** | -0.24 | (-0.4553, -0.0325) | $1.47 \times 10^{-01}$ |
| **GP19** | 0.04 | (-0.0215, 0.0990) | $5.92 \times 10^{-01}$ |
| **GP20** | 0.55 | (-0.4580, 1.6736) | $5.92 \times 10^{-01}$ |
| **GP26** | 0.14 | (-0.0061, 0.2606) | $3.02 \times 10^{-01}$ |
| **GP32** | 0.24 | (0.1072, 0.3757) | $6.62 \times 10^{-03}$ |
| **GP34** | 0.04 | (0.0078, 0.0728) | $7.83 \times 10^{-02}$ |

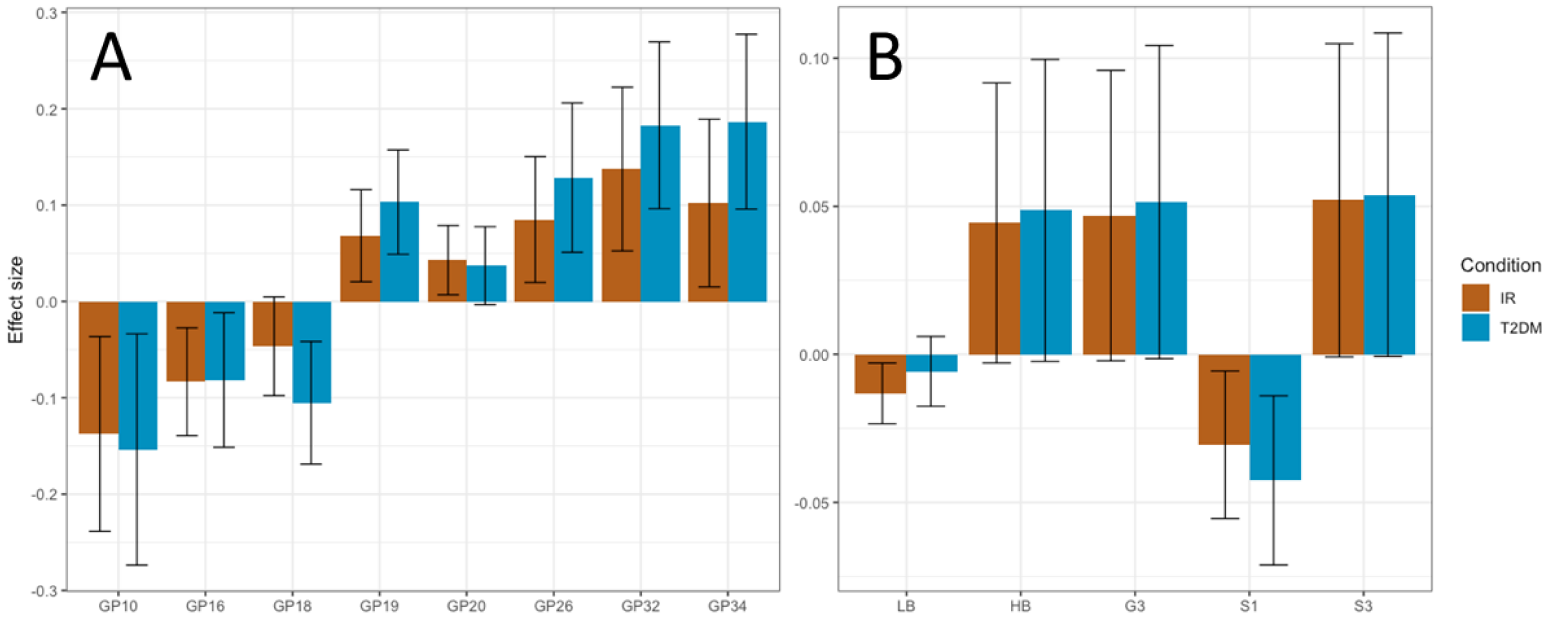


**Supplementary Figure 1 Individual effects of T2DM and IR development on the identified significantly differentiated initial (A) and derived plasma N-glycan traits (B) from the TwinsUK cohort.** Calculated effect size (natural logarithm of difference in relative area) of each presented initial or derived trait is shown on the y axis with error bar representing the 95% confidence interval, while glycan trait name is displayed on the x axis. (GP – glycan peak, LB – low branched glycans, HB – high branched glycans, G3 – trigalactosylated glycans, S1 – monosialylated glycans, S3 – trisialylated glycans)

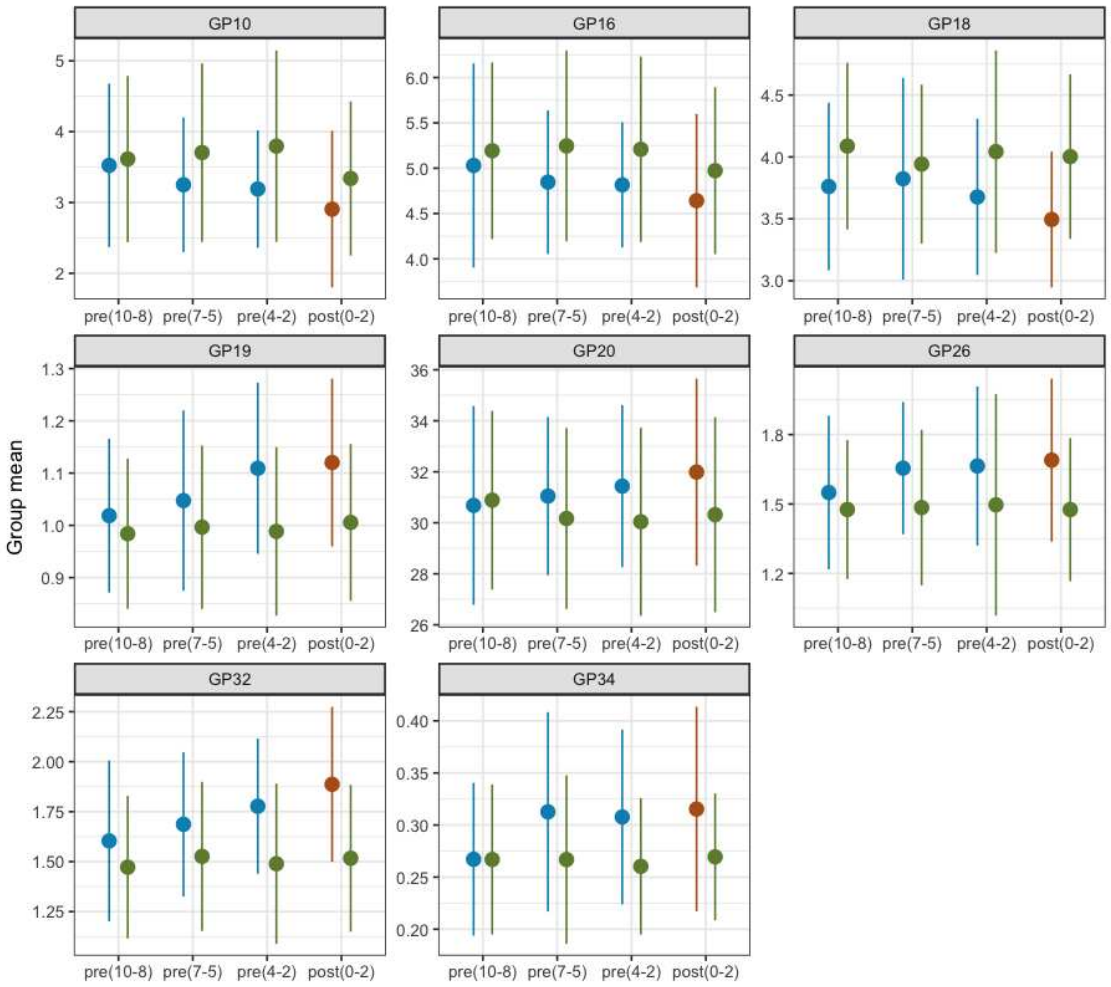


**Supplementary Figure 2 Time-to-diagnosis behaviour of the most significantly altered initial glycan traits in individuals who developed IR/T2DM compared with the control group of the corresponding age for each timepoint from the TwinsUK cohort**. Glycan abundances are presented on the y axis with dots representing calculated means and lines representing 95% confidence intervals, while different temporal groups are presented on the x axis. The timepoint period in which the disease diagnosis occurred is labelled brown, while all pre-diagnosis timepoint periods are labelled blue. Glycan levels of control groups are labelled green. Numbers listed inside the brackets represent years of distance from diagnosis.

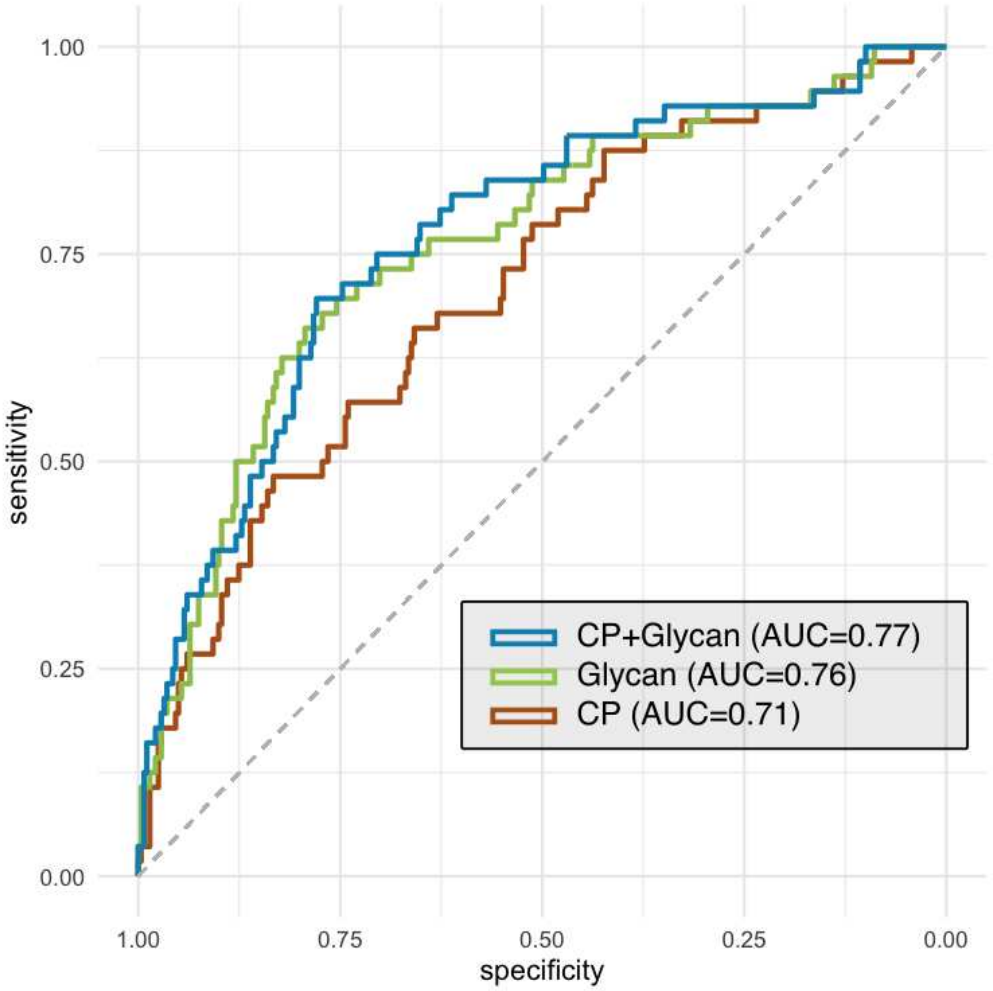


**Supplementary Figure 3 Stratification performance of IR/type 2 diabetes prediction models created from the available TwinsUK cohort data.** Comparison of prediction model based on glycan peaks independently associated with IR/type 2 diabetes (labelled green) with the model including the BMI, smoking status and blood pressure data alone (grouped as risk factors, labelled brown) and the model combining both mentioned risk factors and glycan data (labelled blue).

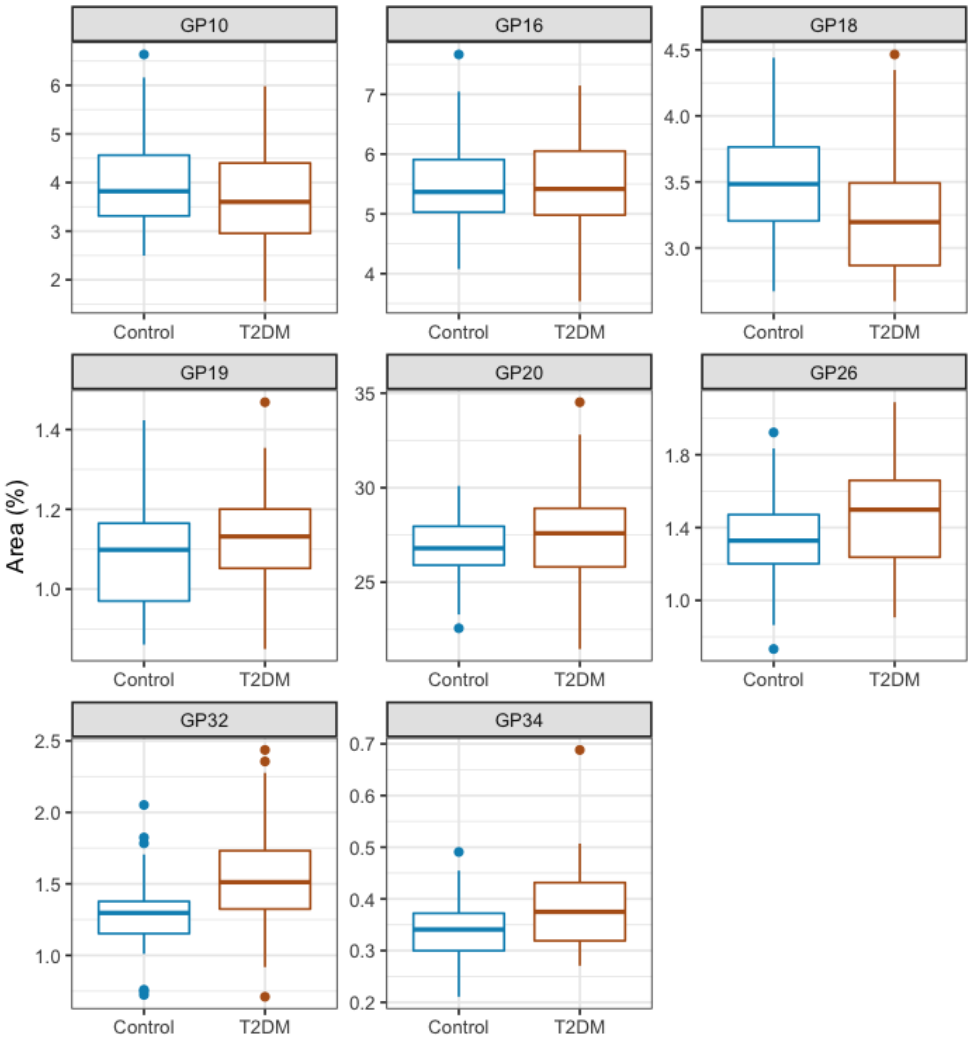


**Supplementary Figure 4 Significant plasma protein N-glycan alterations externally validated on FINRISK confirmation cohort displayed with boxplots.** Y axis represents the glycan abundances of FINRISK participants at baseline sampling. Participants who developed T2DM during follow-up are labelled brown. Participants who remained unaffected at follow-up sampling are labelled blue. Boxes in the boxplot are ranging from 25th to 75th percentile with the median represented as a line inside the box. The whiskers of the boxplot extend from both percentiles, 75th percentile for upper whisker and 25th for lower whisker, to the values within 1.5xIQR. IQR is the inter-quartile range, the distance from the first to the third quartile. Data outside the whiskers' ends are outliers and are plotted individually.